Research article

Multilayer corrosion-resistant material based on iron–carbon alloys

Vladimir A. Grachev [a,*], Andrey E. Rozen [b], Yury P. Perelygin [b], Sergey Yu. Kireev [b], Irina S. Los [b]

[a] A.N. Frumkin Institute of Physical Chemistry and Electrochemistry, Russian Academy of Sciences, 31 bldg 4, Leninsky Prospect, Moscow, 199071, Russia
[b] Penza State University, 40, Krasnaya St., Penza, 440026, Russia

ARTICLE INFO

ABSTRACT

In this study, the architecture of a multilayer metallic material of iron-carbon alloys with an internal protector was developed based on theoretical studies. The operability of the proposed architecture was experimentally verified using gravimetry and electrochemical analysis. The internal position of the protector enabled the modification of the mechanism of corrosion. The stages of corrosion of the multilayer material were revealed; the material was observed as useable until the third layer was perforated. To demonstrate the obtained results, the authors conducted a set of experiments using X-ray microscopy and scanning electron microscopy with an electron probe analysis of the chemical composition. The cost of the developed material is within the same range as widely used corrosion-resistant stainless austenite steels; and in terms of corrosion resistance, this material is comparable to palladium, molybdenum, nickel, and Hastelloy.

1. Introduction

Equipment for the oil and gas industry, shipbuilding, heat-generating industry, and nuclear power systems has been produced from carbon, low-, medium-, and high-alloy steels. These steels constitute between 85–95% of all metal consumption by the industries; this is not going to change in the future [1, 2]. Wide application of steels depends on the availability of raw materials, a developed network of large steel manufacturers as well as good mechanical, engineering, and operational properties. The possibility of controlling the structure through alloying, pressure shaping, and thermal treatment, and the possibility of producing permanent joints using industrial welding at a relatively low cost of materials allows the wide applicability of steel.

A major limitation of steel applications is its relatively low corrosion resistance compared with titanium-, nickel-, and copper-based alloys.

Depending on the composition of aggressive mediums, the operational lifetime of metallic structures does not generally exceed 30 years; in the oil and gas industry, the period is 18 months at most. The operational lifetime can be increased by applying widely available inexpensive materials based on iron-carbon steels; however, this aspect requires further development and remains an urgent task both in terms of theory and practice.

Double-layer steels are widely used to manufacture reservoirs, heat exchangers, reactors, regenerators, air coolers, etc. These steels consist of a cladding layer that is in contact with the aggressive medium and fabricated from a high-alloy corrosion-resistant steel or alloy, and the main layer fabricated from a less expensive carbon or low-alloy steel. The operational lifetime of such bimetal steels depends on the thickness of the cladding layer, and their structural strength is determined by the main layer. The development of innovative corrosion-resistant steels and alloys follows the trend in the increasing content of alloying elements, primarily nickel, chromium, and molybdenum, and the increasing degree of clarification [3, 4]. However, this option has been virtually exhausted because any increase in the electrochemical potential of such materials inevitably intensifies the pitting corrosion, which can lead to perforations of exceptionally small sizes.

In addition to double-layer steels, another type of multilayer corrosion-resistant alloys was developed and patented. These include a layer made of highly corrosion-resistant materials such as molybdenum, wolfram, rhenium, ruthenium, platinum, gold, and silver. This layer is in contact with the aggressive medium. The main layer of such alloys consists of low-carbon and stainless steels, titanium, aluminium, copper, nickel, and their alloys. Such alloys have a third layer, known as the intermediate layer, which provides the alloy with processing plasticity and consists of copper, silver, tantalum, and nickel alloys. Materials with such a composition are frequently expensive owing to the presence of rare and precious metals and have poor technical properties because making their connection permanent using arc welding is impossible [5, 6, 7].

Therefore, the authors designed a new class of multilayer corrosion-resistant materials with an internal protector [8]. They increased the corrosion resistance by laminating the structure of materials containing components with different electrochemical potentials; thus, the corrosion process was split into separate stages, which considerably decreased the rate of through corrosion. The methods of testing the corrosion resistance of such materials were described in detail in [9], and enable predicting the behaviour of the materials in aggressive media and their operation life. At the same time, the principle of corrosion protection embedded into the architecture of multilayer corrosion-resistant materials is based on the well-known processes and phenomena widely applied in materials science and electrochemistry.

This study aimed to develop an architecture of multilayer corrosion-resistant materials based on iron-carbon steels and to analyse their behaviour in aggressive media.

2. Materials and methods

The scientific approach based on the theory of electrochemical processes and the combination of layers fabricated from well-known steel grades facilitates the development of composite materials with increased corrosion resistance [8]. The increased corrosion resistance is ensured by the transition of the process from pitting corrosion in the external layer in contact with the aggressive medium to the anodic dissolution of the subsequent second layer (the protector). The composition of the third layer, which is in contact with the protector, is similar to that of the external one. The composition of the layers depends on the composition of the medium and stationary electrochemical potentials of the metals comprising the layers in this medium. This approach is novel because the protector is located between the layers to be protected. Four-layer compositions were suggested to be applied to items operating under heavy loads; the required strength of such materials is ensured by the composition and thickness of the fourth layer.

Figure 1 shows corrosion in a four-layer material. The material of the first (external) layer (denoted as '1' in the figure) is steel with a sufficiently high corrosion resistance in a specific medium.

At the first stage of corrosion resulting from the interaction between the medium and the external layer, centres of pitting corrosion (7) appear; in time, they grow deeper throughout the external layer [10, 11, 12]. The option of steel for layer 2 is fabricated such that its electrochemical potential would be more negative than that of the first-layer steel upon contact with the medium.

When single pits (6) reach the second layer, the second stage begins, which consists of the interaction between the medium, material of the external layer, and the protector. This process also evokes a contact potential difference between the metals of layers 1 and 2. The steels of the second and first layers become anodic and cathodic, respectively. The contact potential difference ensures cathodic protection of the external layer. Upon the formation of a cavity (5) in the protector, anodic dissolution occurs. The size of the cavity depends on numerous factors, such as

the ratio between the electrochemical potentials of the layers material, temperature, and composition of the medium.

At the third stage, when the protector dissolves down to the third layer (3), the latter also becomes cathodic. The function of the fourth layer (4) is similar to that of the main layer of two-layer steels, which is to provide mechanical strength. Therefore, the rate of the through damage decreases due to the replacement of the cladding layer of two-layer steels by the three-layer component. The integrity of the four-layer composite is demonstrated by the absence of pits in the third layer.

In various media, low-carbon steels are characterized by more negative potential than that of high-alloy steels of austenite, ferrite, and duplex classes [13, 14]. In this regard, it is reasonable to use the steels 10Kh18T, 12Kh18N10T, 08Kh18N10T, 10Kh17N13M2T or their Russian and foreign counterparts, such as AISI304, AISI316, AISI321, and AISI316Ti, as the first (external) and third layers. Low-carbon steels 10, 15, and 20 or their Russian and foreign counterparts, such as AISI1010, AISI1015, and AISI1020, can be used as the second (protective) layer. Low-alloy steels, such as 09G2S, and heat-resistant steels, such as 12KhM, or their counterparts can be used as the fourth layer. The selection of a particular architecture should be accompanied by tests of models and samples.

The objects of the study were as follows:

1. To develop an architecture for multilayer corrosion-resistant materials based on iron-carbon alloys that can ensure corrosion corresponding to the aforementioned stages.
2. To analyse the electrochemical behaviour of the material of the layers in various media and at various temperatures to validate the architecture by tests and experiments.
3. To assess the corrosion resistance of the developed multilayer material and compare it with high-alloy stainless steel.

3. Experimental part

The proposed architecture of the multilayer corrosion-resistant materials was substantiated by using three- and four-layer samples of 12Kh18N10T + Steel 10 + 12Kh18N10T and 08Kh18N10T + Steel 10S + 08Kh18N10T + 09G2S. Note that the steels 12Kh18N10T and 08Kh18N10T are austenitic and have different mechanic properties.

The electrochemical behaviours of the materials of the layers were studied in various media and at various temperatures using the device described in [15]. Metallic plates with a surface area of $2.0\,cm^2$ were used as electrodes. The plates were fabricated from components of the multilayer material, namely Steel 10 and 08Kh18N10T. A 0.5-M solution of iron (III) chloride at $25 \pm 0.5\,°C$ was used as the electrolyte. In the composed galvanic corrosion cell, the electrochemical potentials of the electrodes were measured without circuit current and at various current intensities up to the current of an actual short-circuited galvanic cell. Figure 2 shows the electrochemical potentials of a silver chloride electrode for Steels 10 and 08Kh18N10T as a function of the current strength in a corrosion galvanic cell.

Similar studies were performed in 0.1-M solutions of hydrochloric acid (pH = 1), sodium chloride (pH = 7), and sodium hydroxide (pH = 13) at 25 and 35 °C. The obtained current strength values were used to calculate the mass corrosion index of the protector according to Faraday's law:

$$K_{mass}^- = \frac{m}{S \cdot \tau} \tag{1}$$

$$m = kI\tau = \frac{AI\tau}{nF} \tag{2}$$

$$K_{mass}^- = \frac{AI}{nFS} \tag{3}$$

where K_{mass}^- is the mass corrosion index, m is the mass of the dissolved metal from the surface S in the time τ, k is the electrochemical equivalent
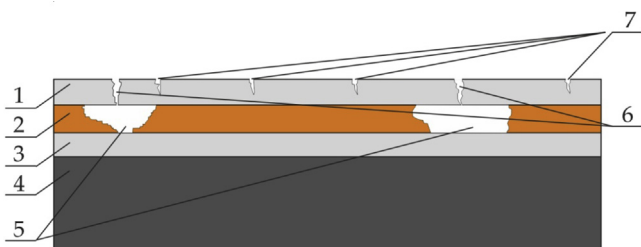

Figure 1. Schematic view of corrosion in a four-layer material: *1* – external layer in contact with the working medium; *2* – internal protector; *3* – third layer; *4* – base layer; *5* – cavities in the protector; *6* – pits through which the aggressive medium interacts with the protector; and *7* – pits with retarded growth owing to the electrochemical effect of the protector.
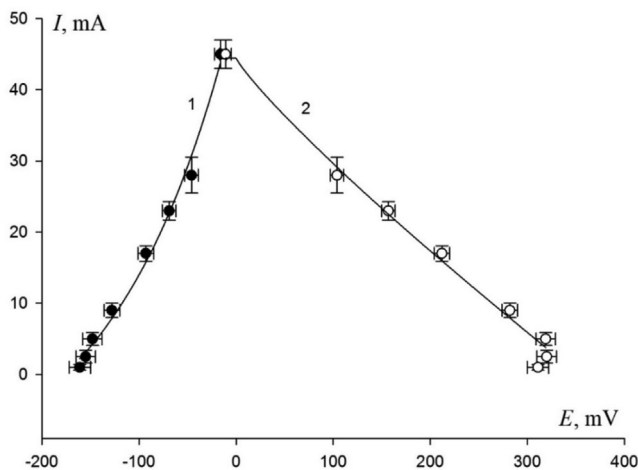
Figure 2. Correlation of electrochemical potentials of steel 10 (line 1) and 08Kh18N10T (line 2) to the current strength (the potentials relate to a silver chloride electrode).

of the internal protector metal, I is the current strength of the short-circuit galvanic cell of the corrosion system, A is the molar mass of the internal protector metal, n is the number of electrons participating in the elementary electrochemical action, and F is the Faraday constant (26.801 A·h/mol).

Temperature dependence of the mass corrosion index enabled the Arrhenius-type effective activation energy to be assessed:

$$K^-_{mass(T_1)} = A \cdot e^{-E_a/RT_1} \tag{4}$$

$$K^-_{mass(T_2)} = A \cdot e^{-E_a/RT_2} \tag{5}$$

$$\frac{K^-_{mass(T_2)}}{K^-_{mass(T_1)}} = \frac{e^{-E_a/RT_2}}{e^{-E_a/RT_1}} = e^{-E_a \Big/ R\left(\frac{1}{T_1} - \frac{1}{T_2}\right)} \tag{6}$$

where $K^-_{mass(T_1)}$ and $K^-_{mass(T_2)}$ are the mass corrosion indices at temperatures T_1 and T_2, respectively, A is the pre-exponential factor, e is the base of the natural logarithm, E_a is the activation energy, and R is the gas constant (8.314 J/mol·K).

In addition, the protector action was assessed using a bimetallic sample of 12Kh18N10T + Steel 10 obtained using explosive welding. Figure 3 shows a cell with the sample immersed in a 0.5-M solution of sodium chloride.
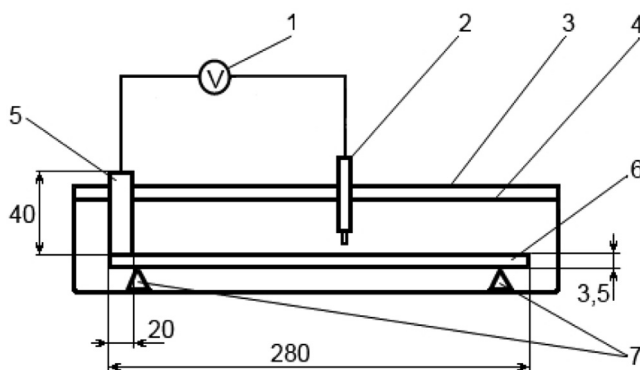
A silver chloride electrode was placed in the cell for further measurements of the sample potential. The potential was measured using an MS8260E digital high-resistance voltmeter with an accuracy of ±1 mV. The distance between the capillary end of the electrode and the stainless steel plate was 3 mm. During the experiment, the position of the reference electrode was changed by moving the electrode a certain distance (x) along the stainless steel plate. Each time the position of the reference electrode was changed, the system was held for 3 ± 0.5 s until the new readings were steady, and then the potential was recorded. The experiment was performed in the glass reservoir with a capacity of 2 L at a constant temperature of 27 ± 0.5 °C. The obtained dependence is shown in Figure 3.

The tangent line method was employed to quantitatively evaluate the internal protector action radius (Figure 4).

4. Results and discussion

The obtained current strength of the short-circuit galvanic cell (Figure 4) enabled the mass index of corrosion to the anode (Steel 10) to be calculated. In 6% aqueous solution of iron (III) chloride at 25 °C, the value was 235 g/m²·h. The mass corrosion indices (calculated using Equation 3) in 0.1-M solutions of hydrochloric acid, sodium chloride, and sodium hydroxide were 1.74, 0.35, and 0.14 g/(m²·h), respectively. As the pH of the solution increased, the rate of protector corrosion decreased. The dependency of K_{mass} from pH at 25 and 35 °C can be described by the following formulae, respectively:

$$K_{mass} = 0.058 + \frac{1.686}{pH} \tag{7}$$

$$K_{mass} = 0.041 + \frac{1.193}{pH} \tag{8}$$

A temperature increase from 25 (curve 1) to 35 °C (curve 2) in the considered pH range led to an increase in the protector's corrosion rate (Figure 5). The activation energy of this process calculated using the Arrhenius equation (Equation 6) was 26.4 kJ/mol, which was indicative of a mixed diffusion-kinetic mechanism of the protector's corrosion [16, 17].

The prediction of the protection should be based on the regularities of the potential distribution over the protected surface, which is determined by a combination of several factors: geometrical parameters of the protector and protected item, electrical conductance of the corrosion
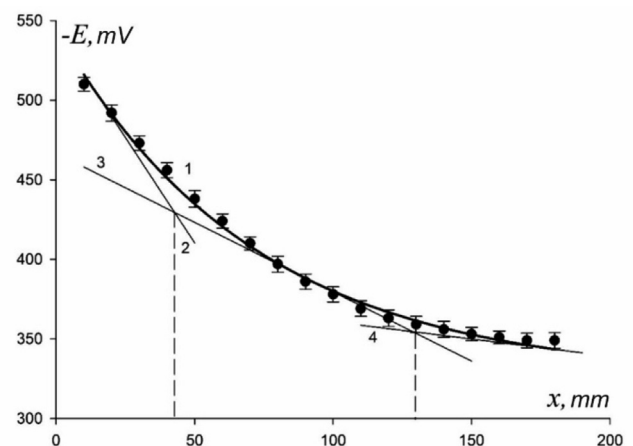

Figure 3. Cell with the sample during the determination of the protector active radius: 1 – high-resistance voltmeter; 2 – silver chloride reference electrode; 3 – cell; 4 – solution level; 5 – Steel 10; 6 – Steel 12Kh18N10T; and 7 – chemically inert supports.

Figure 4. 1 – sample potential (E) of the multi-layer material (with reference to a silver chloride electrode) as a function of the distance (x) between the capillary of the electrode and the protector in a 0.5-M solution of sodium chloride; 2–4 – tangent lines.
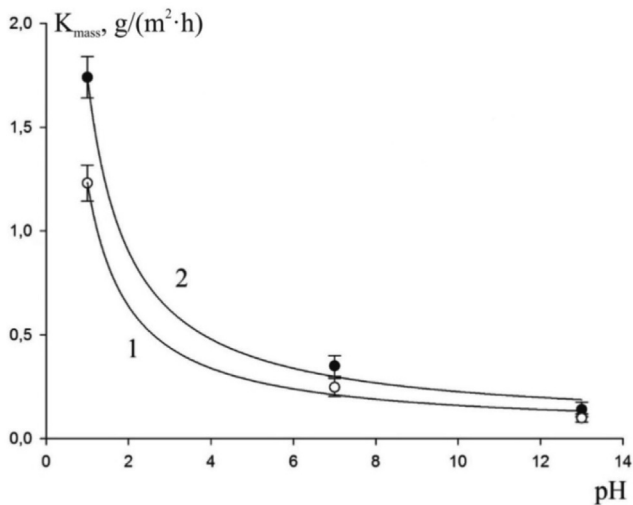
Figure 5. Mass corrosion index of Steel 10 in contact with Steel 08Kh18N10T as a function of pH at 25 (curve 1) and 35 °C (curve 2).

medium, composition of the corrosion medium (pH, anion, or cation composition), etc. [18, 19].

The variation in the distance from the protector to the electrode capillary in a 0.5-mol/L solution of sodium chloride resulted in a displacement of the electrode potential to the region of less negative values (Figure 4). The tangent lines indicated that the most dramatic changes in the electrochemical potential value appeared in the range between 0 and 50 mm. Outside the range, the potential values changed less radically. The cross point of tangent lines 2 and 3 corresponded to x = 42 mm.

The above-mentioned methods, while describing the corrosion mechanism in more detail and proving the protector's efficiency, cannot be used to quantitatively assess the rate of damage to the layers of a multilayer material in the presence of through damage to the external layer. Corrosion to the multilayer's metallic material with pitting in the external layer occurs under different concentrations and diffusion conditions. During the anodic dissolution of the internal protecting layer and lens growth, the medium composition changes due to the dissolution of the protector and the increase in the thickness of the diffusion layer (l), defined as the distance between the surface of the external layer and the protector's wall (Figure 6). This should lead to a decrease in the dissolution rate of the protector and an increase in dissolution rate of the
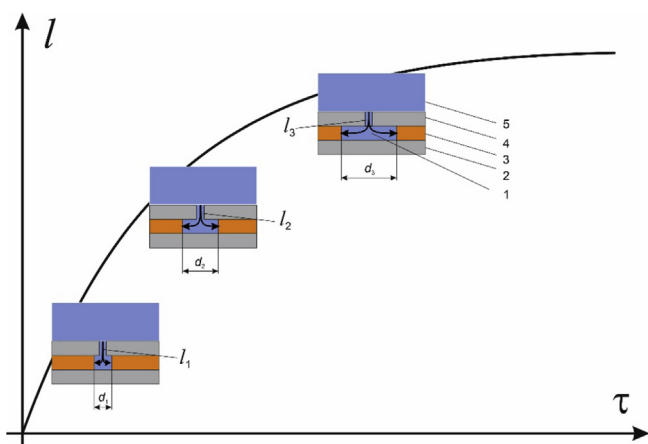

Figure 6. Thickness of the diffusion layer (l) as a function of exposure time (τ) at various diameters (d) of the lens in the middle layer: 1 – lens, 2 – the third layer, 3 – the second layer (internal protector), 4 – the first layer, and 5 – corrosion medium.

external layer, that is, to the formation of new pits. The diffusion and kinetic control of the corrosion is demonstrated by the above-mentioned activation energy value.

To simulate all stages of the process of corrosion to multilayer materials, the authors propose a rapid test on detachable samples [20]. During the test, the authors assessed the rate of corrosion to each layer. In addition, the existence of the pitting-induced perforations and the integrity of the third layer was monitored, which enabled the operability criterion of the four-layer composite to be formulated.

Using this procedure, the corrosion resistance of the outer, inner, and lower layers was determined in a 6% aqueous solution of iron (III) chloride given that the diameter of the artificial pitting in the outer layer was 1 mm and the diameter of the artificial lens in the protector layer varied from 3 to 20 mm. The following was established:

- The rate of the protector dissolution decreases if the lens diameter in the protector is increased. If the protector lens diameter exceeds 15 mm, a dramatic decrease in the rate of the protector dissolution is observed, which is related to the fact that, in such a scenario, the corrosion agent of the medium has difficulty in reaching the protector material. Additionally, the rate of dissolution of the outer layer can be assumed to not depend on the lens diameter and it is in the range between 0.22 and 0.25 g/m^2·h.
- If the protector lens diameter is less than 20 mm, the third layer does not dissolve.
- The rate of corrosion of separate plates fabricated with high-alloy steel and placed in a 6% solution of iron (III) chloride is between 58 and 66 times higher than that of identical plates as part of a multilayer material, which proves the effectiveness of the protector.
- The rate of corrosion of a protector plate fabricated from carbon steel and placed in a 6% solution of iron (III) chloride is between 35 and 220 times higher than that of an identical plate as part of a multilayer material, which is a result of diffusion limitations or insoluble corrosion.
- In a 6% solution of iron (III) chloride, the corrosion resistance of the designed multilayer material 12X18H10T + Steel 10 + 12X18H10T exceeds that of high-alloy stainless steel 12X18H10T by 21.9 times

The set of the assessment criteria and tests used to assess the corrosion behaviour of the multilayer metallic materials with an internal protector enabled the authors to demonstrate the effectiveness and good performance of the multilayer, corrosion-resistant architecture.

The obtained results were verified with a set of tests involving X-ray microscopy using an XRadia Versa XRM-500 and scanning electron microscopy (SEM) investigation with an electron probe analysis of chemical composition using an FEL Helios Nanolab 660/FEL Versa 3D.

Three- and four-layer samples with internal protectors were manufactured using explosion wielding (their architecture is described above). The samples were then submerged into a corrosion medium (6% solution of iron (III) chloride). The tests did not involve artificial pitting; corrosion occurred naturally. X-ray microscopy verified the mechanism of corrosion to multilayer metallic materials with an internal protector. The mechanism involves pitting corrosion of the first layer (Figure 7a) transferring into contact corrosion (Figure 7b) and then occurring only in the second, or protector, layer for a long time (Figure 7c). The wave-like structure of the lines between the layers formed by explosion welding did not affect the visualization of the binary model and corresponded perfectly with the results of the gravimetric measurements. The deviation between the test results and calculated values obtained from the binary model was 0.7% or less.

An analysis of the composition of the corrosion zone (Figure 8) demonstrated that the composition of the inner surface of the lens changed and also indicated that low-carbon Steel 10 elements dominated oxidation (spots 2, 3, and 4).

Tables 1 and 2 below show the chemical composition at each of the spots marked at the surface of the sample (Figure 8b).
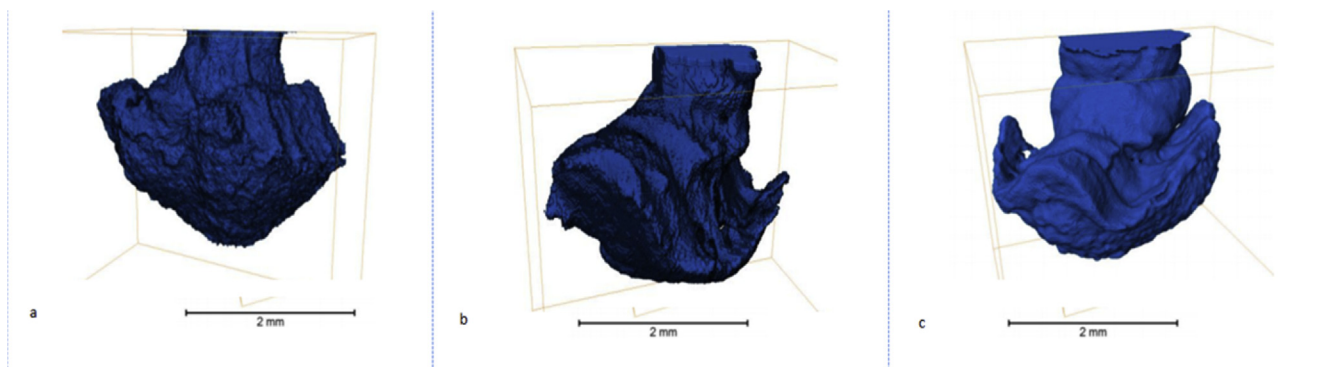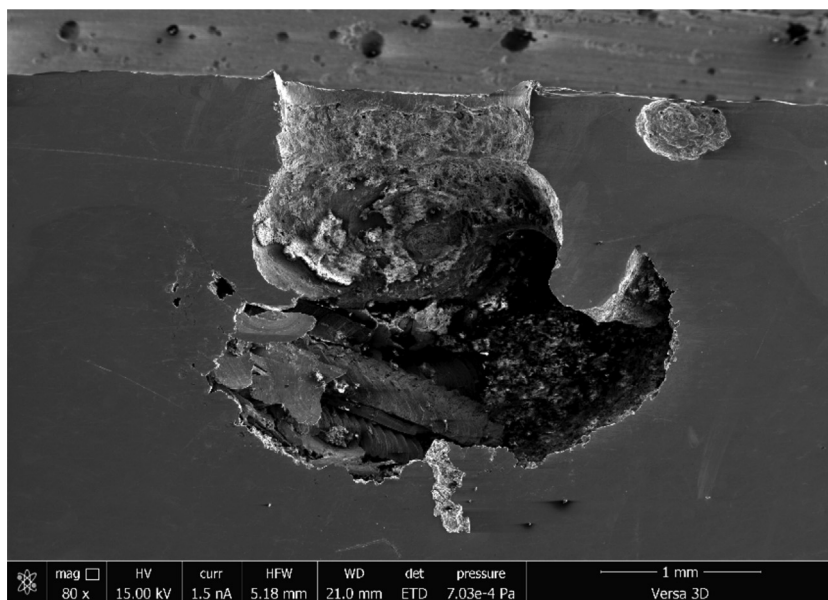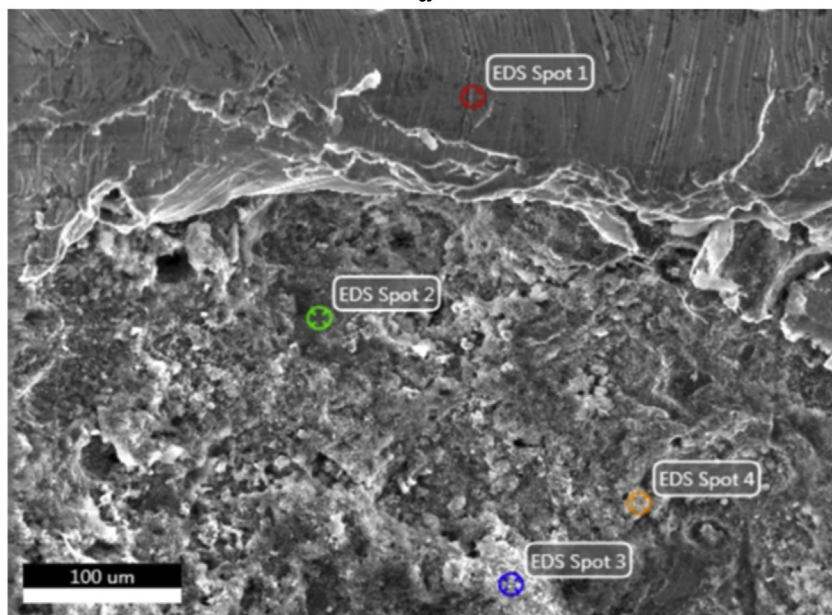
Figure 7. 3D visualization of the binary model of corrosion to a three-layer material with an internal protector (12X18H10T + Steel 10 + 12X18H10T) at (a) 72 h, (b) 168 h, and (c) 360 h in a 6% solution of iron (III) chloride.

Figure 8. (a) SEM image of the corrosion zone used to compose (b) a distribution profile of chemical composition in spots at the surface of the sample.

Table 1. Weight percentage of various elements at the spots.

Weight %	Fe	Cr	Ni	O	C	Mn	Si	Ti	Ca	P	S	Na
Spot 1	67.52	17.45	7.61	3.27	1.4	1.17	1.01	0.51	0.04	0	0	0
Spot 2	54.6	14.91	6.35	9.09	8.45	1.16	0.42	4.06	0.28	0.4	0.27	0
Spot 3	40.05	12.88	7.08	16.67	9.63	0.54	1.37	9.84	0.57	0.86	0.39	0
Spot 4	30.09	10.71	5.09	24.32	11.46	0	1.66	12.93	0.44	1.75	0.56	0.48

Table 2. Percentage of nuclides of various elements at the spots.

Nuclear %	Fe	Cr	Ni	O	C	Mn	Si	Ti	Ca	P	S	Na
Spot 1	58.56	16.25	6.28	9.91	5.65	1.04	1.75	0.52	0.05	0	0	0
Spot 2	47.35	10.26	3.87	20.34	25.17	0.76	0.54	3.04	0.25	0.47	0.3	0
Spot 3	22.06	7.62	3.71	32.05	24.67	0.3	1.5	6.32	0.44	0.86	0.37	0
Spot 4	14.33	5.48	2.31	40.43	25.39	0	1.57	7.18	0.29	1.51	0.46	0.56

5. Conclusions

In this study, an architecture of multilayer corrosion-resistant materials based on iron-carbon alloys was developed. Its operability was confirmed experimentally.

The electrochemical behaviour of materials of the layers was analysed in various media and at various temperatures. The mass corrosion index of materials of the layers was determined in various media. The activation energy of the protector's dissolution was determined, which confirmed the diffusion and kinetic nature of the phenomenon.

A model for the corrosion behaviour of multilayer metallic materials with an internal protector was developed, which was verified by the results of X-ray microscopy and SEM investigation.

The cost of the developed material is within in the range group as widely used corrosion-resistant stainless austenite steels; and in terms of corrosion, this material is comparable to palladium, molybdenum, nickel, and Hastelloy [21].

Declarations

Author contribution statement

Vladimir A. Grachev: Conceived and designed the experiments; Wrote the paper.

Andrey E. Rozen: Conceived and designed the experiments; Contributed reagents, materials, analysis tools or data.

Yury P. Perelygin, Sergey Y. Kireev, Irina S. Los: Performed the experiments; Analyzed and interpreted the data.

Funding statement

Competing interest statement

The authors declare no conflict of interest.

Additional information

No additional information is available for this paper.

References

[1] G.N. Elanskii, A.E. Semin, S.N. Paderin, S.I. Shakhov, L.N. Shevelev, Results of 14th steelmakers congress, Metallurgist 1 (2017) 29–45.

[2] A.M. Nemenov, Events in figures and facts, Metallurgist 7 (2017) 95–104.

[3] A.A. Pavlov, Development of new corrosion-resistant bimetals with increased corrosion resistance prepared by electroslag surfacing technology, Chem. Petrol. Eng. 53 (7-8) (2017) 551–556.

[4] D.C. Agarwal, Nickel base alloys and newer 6Mo stainless steels meet corrosion challenges of the modern day chemical process industrie, Anti-Corros. Methods Mater. 48 (5) (2001) 287–297.

[5] Y.S. Kim, J.G. Park, B.S. An, Y.H. Lee, C.W. Yang, J.G. Kim, Investigation of zirconium effect on the corrosion resistance of aluminum alloy using electrochemical methods and numerical simulation in an acidified synthetic sea salt solution, Materials 11 (10) (2018) 1982.

[6] M.-S. Hong, Y. Park, J.G. Kim, K. Kim, Effect of incorporating MoS2 in organic coatings on the corrosion resistance of 316L stainless steel in a 3.5% NaCl solution, Coatings 9 (1) (2019) 45.

[7] O.R. Bergmann, V.M. Felix, W.J. Simmons, R.H. Tietjen. Patent No. US5323955. Jun. 28, 1994. Explosively bonding metal composite. Available at: https://patent images.storage.googleapis.com/f7/f6/58/b16e7afbf93935/US5323955.pdf

[8] Yu.P. Perelygin, A.E. Rosen, I.S. Los, S.Y. Kireev, A new corrosion-resistant multilayer material, Prot. Met. Phys. Chem. Surf. 50 (7) (2014) 856–859.

[9] V.A. Grachev, A.E. Rozen, Yu.P. Perelygin, S.Y. Kireev, I.S. Los', A.A. Rozen, Measuring corrosion rate and protector effectiveness of advanced multilayer metallic materials by newly developed methods, Heliyon 4 (8) (2018), e00731.

[10] J. Shi, D. Wang, J. Ming, W. Sun, Passivation and pitting corrosion behavior of a novel alloy steel (00Cr10MoV) in simulated concrete pore solution, J. Mater. Civ. Eng. 30 (10) (2018).

[11] B. Zhang, Y. Zhang, S.M. Guo, A thermodynamic study of corrosion behaviors for CoCrFeNi-based high-entropy alloys, J. Mater. Sci. 53 (7) (2018) 1–10.

[12] M. Djama, D. Saidi, A. Kadri, N. Kherrouba, B. Mehdi, S. Mathieu, T. Schweitzer, I. Brahim, Correlation between the pitting potential evolution and σ phase precipitation kinetics in the 2205 duplex stainless steel, J. Mater. Eng. Perform. 27 (8) (2018) 3911–3919.

[13] State Standard GOST 9.005-72, Permissible and Impermissible Contacts with Metals and Non-metals. General Requirements, Gosstandart, Moscow, 1973, p. 28.

[14] V.S. Pakhomov, A.A. Shevchenko, Chemical Resistance of Materials and protection against Corrosion, Khimiya, KolosS, Moscow, 2009, p. 444.

[15] Yu.P. Perelygin, S.Yu. Kireev, I.S. Los, A.E. Rozen, M.Yu. Panin, Installation for electrochemical survey of metal corrosion. Russian patent RU 2533344 C1 (Int. Cl. G01N 17/02). Published on November 20, 2014, Bulletin No. 32, Available at: htt p://www.freepatent.ru/images/img_patents/2/2533/2533344/patent-2533344 .pdf.

[16] F.I. Danilov, V.S. Protsenko, Actual activation energy of electrode process under mixed kinetics conditions, Russ. J. Electrochem. 45 (10) (2009) 1104–1105.

[17] B.N. Mikhailov, O.V. Nemykina, Determination of effective activation energy of corrosion, Polzunovsky Vestnik 3 (2009) 135–137.

[18] I.V. Semenova, G.M. Florianovich, A.V. Khoroshilov, Corrosion and Corrosion protection, Fizmatlit, Moscow, 2006, p. 376.

[19] .Ya. Iossel' Yu, G.E. Klenov, Mathematical Predictions of Electrochemical Corrosion and protection of Metals. Reference Book, Metallurgiya, Moscow, 1984, p. 272.

[20] S.Yu. Kireev, I.S. Los, A.E. Rozen, Yu.P. Perelygin, Procedures for corrosion tests of multilayered metal material, Korroziya: Materialy, Zashchita 8 (2017) 42–47.

[21] A.M. Sukhotin, V.S. Zotikov, Chemical Resistance of Materials. Reference Book, Khimiya, Leningrad, 1975, p. 408.